ON FRACTIONAL SPHERICALLY RESTRICTED HYPERBOLIC DIFFUSION RANDOM FIELD

N.Leonenko*
Cardiff University
Senghennydd Road
CF24 4AG Cardiff, UK
LeonenkoN@Cardiff.ac.uk

A.Olenko†
La Trobe University
Melbourne, Australia
a.olenko@latrobe.edu.au

J.Vaz‡
University of Campinas
IMECC
SP 13083-859 Campinas, Brazil
vaz@unicamp.br

September 28, 2023

Abstract

The paper investigates solutions of the fractional hyperbolic diffusion equation in its most general form with two fractional derivatives of distinct orders. The solutions are given as spatial-temporal homogeneous and isotropic random fields and their spherical restrictions are studied. The spectral representations of these fields are derived and the associated angular spectrum is analysed. The obtained mathematical results are illustrated by numerical examples. In addition, the numerical investigations assess the dependence of the covariance structure and other properties of these fields on the orders of fractional derivatives.

AMS classification: 60G60, 60G15, 60D05, 60K05

Keywords: Spherical random fields, Fractional hyperbolic diffusion equation, Caputo derivative, Fractional telegraph equation, Angular spectrum, Spectral theory, Spatio-temporal data

*FAPEST (BRAZIL) grant, ARC grant DP220101680, LMS grant 42997 (UK)
†ARC grant DP220101680
‡FAPEST (BRAZIL) grant

1 Introduction

Spherical random fields have been used for modelling various phenomena in areas such as earth sciences, for example, in geophysics and climatology [8, 9, 16, 28, 31], and cosmology, see [3, 4, 6, 29] and the references therein. In fact, the application of statistical methods in cosmology [6] has become increasingly important due to the many experimental data obtained in recent years [1]. Spherical random fields are of particular interest for modelling and analysis of Cosmic Microwave Background (CMB) radiation [4, 5, 25, 29]. The CMB is a spatially isotropic radiation field spread throughout the universe, that was originated around 14 billion years ago [12, 37]. It is the main source of information we have about initial phases of the universe. The CMB radiation can be mathematically modelled as an isotropic, mean-square continuous spherical random field, which has a spectral representation by means of spherical harmonics. Consequently, models of temporal spherical random fields, in addition to their innate theoretical interest, have some practical applications in the studies of the CMB radiation evolution.

Such models were recently provided in [3, 4, 25], where stochastic diffusion equations were used to describe changes of the spherical random fields over time. The hyperbolic heat equation is formally identical to the linear telegraph equation presented by Heaviside in his study of transmission lines. It was introduced by Cattaneo [7] to impose a bounded speed of propagation for the temperature disturbances, in contrast with the classical parabolic heat equation, that has an unbounded propagation speed.

While the classical diffusion equation results from the conversation law $u_t + \mathrm{div} q = 0$ and Fick's law $q + k\,\mathrm{grad} u = 0$, Cattaneo equation results from the modification of Fick's law by introducing a term proportional to the first order derivative of the flux q, that is, $\tau q_t + q + k\,\mathrm{grad} u = 0$. If one considers another modification of these equation, replacing the ordinary derivative by fractional derivatives of the Caputo type, see (2) below, then

$$\frac{\partial^\alpha u}{\partial t^\alpha} + \mathrm{div} q = 0, \qquad \tau \frac{\partial^\beta q}{\partial t^\beta} + q + k\,\mathrm{grad} u = 0,$$

and the resulting modified Cattaneo equation is

$$\tau \frac{\partial^\beta}{\partial t^\beta} \frac{\partial^\alpha u}{\partial t^\alpha} + \frac{\partial^\alpha u}{\partial t^\alpha} - k\nabla^2 u = 0. \tag{1}$$

It was shown that for $\alpha + \beta > 1$

$$\frac{\partial^\beta}{\partial t^\beta} \frac{\partial^\alpha u}{\partial t^\alpha} = \frac{\partial^\alpha}{\partial t^\alpha} \frac{\partial^\beta u}{\partial t^\beta} = \frac{\partial^{\alpha+\beta} u}{\partial t^{\alpha+\beta}}$$

if $u(t)$ is analytic and such that, for any $n \in \mathbb{N}$, $|u^{(n)}(0)| < K^n$, for some constant $K > 0$, and $u^{(1)}(0) = 0$. Under these conditions, (1) becomes

$$\tau \frac{\partial^{\alpha+\beta} u}{\partial t^{\alpha+\beta}} + \frac{\partial^\alpha u}{\partial t^\alpha} - k\nabla^2 u = 0.$$

The boundedness of the speed propagation is desirable because the large-scale coherent structures that are observed in the CMB are believed to be the remains of the waves in the plasma universe. In [3] the explicit solution of the model was given in terms of series of elementary functions, and therefore it could be useful for various qualitative and numerical studies. For more details and references on the telegraph equations, or hyperbolic diffusion equation, consult [3, 4, 21, 22, 35], among others.

On the other hand, it is known that deviations from the standard diffusive behavior occur in many situations [2]. Among the various models of anomalous behavior, an important approach is based on fractional differential equations [11, 13]. The calculus of non-integer order called fractional calculus, attracted an increasing interest over the last decades, specially for the modelling of phenomena involving memory effects, see, for example, anomalous transport [11], problems with dissipation [27], etc. However, these models are not unique in the sense that there are numerous non-equivalent definitions of a fractional derivative in the literature.

It is natural at this point to think of Cattaneo's approach to the hyperbolic diffusion equation within the framework of the continuous-time random walk (CTRW). The key point in Cattaneo's approach was to modify the constitute equation (Fick's law) by introducing a term proportional to the first order derivative of the flux. In [10] Compte and Metzler discussed possibilities for the generalization of the Cattaneo equation, and one of these possibilities is to consider the CTRW scenario of fractal time random walk, which gives an equation which can be written in terms of Caputo fractional derivatives in the time variable.

The present paper is a continuation of the line of research of the work [3],[4] and [24]. Our main objective is to study the fundamental solutions to fractional hyperbolic diffusion equation in the time variable using the Caputo derivative, and its properties. The exact solutions of fractional hyperbolic diffusion equations with random initial conditions are derived. Then, the angular spectrum of the solution to the spherical fractional hyperbolic diffusion equations restricted to sphere from homogeneous and isotropic random field is obtained. It is given as a solution of fractional hyperbolic diffusion equation with random random initial conditions under very general assumptions about indexes α and β of fractional equation, namely, $0 < \alpha \leq 1$ and $1 < \alpha + \beta \leq 2$.

Time-fractional telegraph equations with Caputo fractional derivatives and $\beta = \alpha \in (0, 1]$ were considered in [32] and [14], while with Hilfer and Hadamar fractional derivatives in [36]. They provided the Fourier transform of some Cauchy problems for these equations as well as probabilistic interpretations in some specific cases. In the framework of spherical random fields satisfying random initial conditions, the fundamental solution of the hyperbolic diffusion equation were derived in [3] and [4], while the fractional version was investigated in [24] (again only for the case of $\alpha \in (0, 1],\ \alpha = \beta$). Obviously, for Caputo fractional derivatives the results of this paper are more general since it is only assumed that $0 < \alpha \leq 1$ and $1 < \alpha + \beta \leq 2$.

This paper is organized as follows. Section 2 introduces the required notations and the initial-value problem for fractional hyperbolic diffusion equations. Then, it provides various results about the Fourier transforms of the solutions to the equations. The solutions are given using these Fourier transforms as a stochastic integrals. Section 3 investigates restrictions of the solutions to the unit sphere. Specifications of the main results and important particular cases are considered in examples. Section 4 presents simulation studies that illustrate properties of the solutions with respect to orders of fractional derivatives.

All numerical computations and simulations in this paper were performed using the software R version 4.3.1 and Python version 3.11.5. The HEALPix representation for spherical data was used, see `http://healpix.sourceforge.net`. The Python package "healpy" was utilized for the computing Laplace series coefficients to create spherical maps. The R package "rcosmo", see [17] and [18], was employed to visualise the obtained spherical fields. The R and Python code used for numerical examples in Section 4 are freely available in the folder "Research materials" from the website `https://sites.google.com/site/olenkoandriy/`.

2 Fractional Hyperbolic Diffusion Equation

The Caputo fractional derivative of order γ, with $(n-1) < \gamma < n,\ n \in \mathbb{N}$, is defined as

$$\mathrm{D}_t^{\gamma} q(x,t) = \frac{\partial^{\gamma}}{\partial t^{\gamma}} q(x,t) = \frac{1}{\Gamma(n-\gamma)} \int_0^t \frac{q^{(n)}(x,\tau)}{(t-\tau)^{\gamma+1-n}} d\tau, \tag{2}$$

where $q^{(n)}$ denotes the partial derivative of order n of $q(x,t), x \in \mathbb{R}^3,\ t > 0$, and $\Gamma(\cdot)$ is the gamma function. Various properties of Caputo derivatives can be found in [19], [30] and [33].

We consider the hyperbolic diffusion equation

$$\frac{1}{c^2} \frac{\partial^{\alpha+\beta}}{\partial t^{\alpha+\beta}} q(x,t) + \frac{1}{D} \frac{\partial^{\alpha}}{\partial t^{\alpha}} q(x,t) = k^2 \Delta q(x,t), \tag{3}$$

where Δ is the Laplacian in $\mathbb{R}^3$, $0 < \alpha \leq 1$, $1 < \alpha + \beta \leq 2$, $D > 0$, and $c > 0$. The random field $q(x,t) = q(x,t,\omega)$, $\omega \in \Omega$, satisfies the random initial conditions:

$$q(x,t)|_{t=0} = \eta(x), \quad \left. \frac{\partial}{\partial t} q(x,t) \right|_{t=0} = 0, \tag{4}$$

where the random field $\eta(x) = \eta(x,\omega),\ x \in \mathbb{R}^3,\ \omega \in \Omega$, defined on a suitable complete probability space $(\Omega, \mathcal{F}, \mathrm{P})$, is assumed to be measurable, mean-square continuous, wide-sense homogeneous and isotropic with zero mean and the covariance function $\mathrm{Cov}(\eta(x), \eta(y)) = B(\|x-y\|),\ x \in \mathbb{R}^3,\ y \in \mathbb{R}^3$.

The covariance function $B(\cdot)$ has the following representation, see [20, p.12] and [23, p.18],

$$B(\|x-y\|) = \int_{\mathbb{R}^3} \cos(\langle \lambda, x-y \rangle) F(d\lambda) = \int_0^{\infty} \frac{\sin(\mu \|x-y\|)}{\mu \|x-y\|} G(d\mu), \tag{5}$$

for some bounded, non-negative measures $F(\cdot)$ on the measurable space $(\mathbb{R}^3, \mathcal{B}(\mathbb{R}^3))$ and $G(\cdot)$ on $\left(\mathbb{R}^1_+, \mathcal{B}(\mathbb{R}^1_+)\right)$, such that

$$F(\mathbb{R}^3) = G\left([0,\infty)\right) = B(0), \quad G(\mu) = \int_{\|\lambda\|<\mu} F(d\lambda).$$

Then, there exists a complex-valued orthogonal random measure $Z(\cdot) = Z(\cdot, \omega)$, $\omega \in \Omega$, such that for every $x \in \mathbb{R}^3$, the random field $\eta(x)$ has the spectral representation

$$\eta(x) = \int_{\mathbb{R}^3} e^{\mathrm{i}\langle \lambda, x\rangle} Z(d\lambda),\ \mathrm{E}\,|Z(\Delta)|^2 = F(\Delta),\ \Delta \in \mathcal{B}(\mathbb{R}^3). \tag{6}$$

Let $Y_{lm}(\theta, \varphi),\ \theta \in [0, \pi],\ \varphi \in [0, 2\pi],\ l = 0, 1, 2, \ldots, m = -l, \ldots, l$, be complex spherical harmonics defined by the relation

$$Y_{lm}(\theta, \varphi) = (-1)^m \left[\frac{(2l+1)(l-m)!}{4\pi(l+m)!}\right]^{1/2} e^{\mathrm{i}m\varphi} P_l^m(\cos\theta),$$

where $P_l^m(\cdot)$ are the associated Legendre polynomials.

The Bessel function $J_\nu(\cdot)$ of the first k and of order ν is defined by

$$J_\nu(\mu) = \sum_{n=0}^{\infty} \frac{(-1)^n}{n!\Gamma(n+\nu+1)} \left(\frac{\mu}{2}\right)^{2n+\nu}.$$

By the addition theorem for Bessel functions ([20, p.14] and [23, p.20]) and the Karhunen theorem ([23, p.10]):

$$\eta(x) = \pi\sqrt{2} \sum_{l=0}^{\infty} \sum_{m=-l}^{l} Y_{lm}(\theta, \varphi) \int_0^\infty \frac{J_{l+\frac{1}{2}}(\mu r)}{(\mu r)^{1/2}} Z_{lm}(d\mu), \tag{7}$$

where $Z_{lm}(\cdot) = Z_{lm}(\cdot, \omega), \omega \in \Omega$, is a family of complex-valued random measures on $\left(\mathbb{R}^1_+, \mathcal{B}(\mathbb{R}^1_+)\right)$, such that

$$\mathrm{E}[Z_{lm}(\Delta_1)\overline{Z_{l'm'}(\Delta_2)}] = \delta_{ll'}\delta_{mm'} G(\Delta_1 \cap \Delta_2),\ \Delta_i \in \mathcal{B}(\mathbb{R}^1_+),\ i = 1, 2.$$

The stochastic integrals in (6) and (7) are interpreted as $\mathscr{L}_2(\Omega)$ integrals with structural measures F and G respectively.

Let us consider the non-random initial conditions of the form

$$q(x,t)|_{t=0} = \delta(x), \qquad \left.\frac{\partial}{\partial t} q(x,t)\right|_{t=0} = 0, \tag{8}$$

where $\delta(x)$ is the Dirac delta function.

Let $Q(x,t), x \in \mathbb{R}^3, t > 0$, be the fundamental solution (or the Green's function) of the initial-value problem (3) and (8), and let

$$H(\kappa,t) = \int_{\mathbb{R}^3} e^{i\langle \kappa, x\rangle} Q(x,t)dx,\ \kappa \in \mathbb{R}^3,\ t \geq 0, \tag{9}$$

be its Fourier transform.

The tree-parametric Mittag-Leffler function or Prabhakar function, see [19, p. 97] and [15], is defined by

$$\mathrm{E}^{\zeta}_{a,b}(z) = \sum_{k=0}^{\infty} \frac{(\zeta)_k \cdot z^k}{k!\,\Gamma(ak+b)}, \tag{10}$$

where $\zeta > 0,\ \mathrm{Re}(a) > 0, \mathrm{Re}(b) > 0$ and $(\zeta)_k = \Gamma(\zeta+k)/\Gamma(\zeta)$ is the Pochhammer symbol.

The following theorem derives the Fourier transform (9) in terms of the function defined by (10). Later on, this result will be used to obtain the solution $q(x,t,\omega),\ x \in \mathbb{R}^3$, $\omega \in \Omega$, $t \geq 0$, of the initial-value problem (3) with the initial conditions given in (4)

Theorem 1. *The Fourier transform* (9) *of the initial-value problem* (3) *and* (8) *is given by the formula*

$$\begin{aligned} H(\kappa,t) &= 1 + \sum_{n=0}^{\infty} \left(-\left\|\kappa\right\|^2 c^2 t^{\alpha+\beta}\right)^{n+1} \mathrm{E}^{n+1}_{\beta,(\alpha+\beta)(n+1)+1}\left(-\frac{c^2}{D}t^{\beta}\right) \\ &= 1 - \left\|\kappa\right\|^2 c^2 t^{\alpha+\beta} \sum_{m=0}^{\infty}\sum_{n=0}^{\infty} \binom{m}{n} \frac{\left(-\frac{c^2}{D}t^{\beta}\right)^m \left(\left\|\kappa\right\|^2 D t^{\alpha}\right)^n}{\Gamma(\beta m + \alpha n + \alpha + \beta + 1)}, \end{aligned}$$

where $1 < \alpha+\beta \leq 2,\ 0 < \alpha \leq 1,\ x \in \mathbb{R}^3,\ t \geq 0.$

Proof. The Fourier transformed version of (3) is

$$\frac{1}{c^2}\frac{\partial^{\alpha+\beta}}{\partial t^{\alpha+\beta}} H(\kappa,t) + \frac{1}{D}\frac{\partial^{\alpha}}{\partial t^{\alpha}} H(\kappa,t) = -\left\|\kappa\right\|^2 H(\kappa,t)$$

with

$$H(\kappa,0)=1,\quad \frac{\partial H(\kappa,0)}{\partial t}=0. \tag{11}$$

Let $\tilde{H}(s)=\mathcal{L}[H(\kappa,t);s]$ denotes the Laplace transform of $H(\kappa,t)$. Then, using [14, (4.8)] one obtains

$$\tilde{H}(s)=\frac{s^{\alpha+\beta-1}+c^2D^{-1}s^{\alpha-1}}{s^{\alpha+\beta}+c^2D^{-1}s^{\alpha}+\|\kappa\|^2c^2}=\frac{1}{s}-\frac{\|\kappa\|^2c^2}{s(s^{\alpha+\beta}+c^2D^{-1}s^{\alpha}+\|\kappa\|^2c^2)}.$$

For s such that

$$\left|\frac{\|\kappa\|^2c^2}{s^{\alpha+\beta}+c^2D^{-1}s^{\alpha}}\right|<1 \tag{12}$$

it can be written as

$$\tilde{H}(s)=\frac{1}{s}+\sum_{n=0}^{\infty}\left(-\|\kappa\|^2c^2\right)^{n+1}\frac{s^{-\alpha(n+1)-1}}{(s^{\beta}+c^2D^{-1})^{n+1}}.$$

It is known [19, (5.1.33)] that

$$\mathcal{L}\left[t^{b-1}\mathrm{E}_{a,b}^{\zeta}(-\mu t^a);s\right]=\frac{s^{a\zeta-b}}{(s^{\alpha}+\mu)^{\zeta}},$$

where the function $\mathrm{E}_{a,b}^{\zeta}$ is defined by (10).

Using the substitution

$$a=\beta,\quad b=(\alpha+\beta)(n+1)+1,\quad \zeta=n+1,$$

one can write $H(\kappa,t)=\mathcal{L}^{-1}[\tilde{H}(s);t]$ as

$$H(\kappa,t)=1+\sum_{n=0}^{\infty}(-\|\kappa\|^2c^2t^{\alpha+\beta})^{n+1}\mathrm{E}_{\beta,(\alpha+\beta)(n+1)+1}^{n+1}(-c^2D^{-1}t^{\beta}).$$

It follows by Lerch's theorem that $H(\kappa,t)$ has the Laplace transform $\tilde{H}(s)$ not only for the range given by (12), but also for all values of s.

The above expression for $H(\kappa, t)$ can be rewritten in a form that is convenient for numeric computations. Using (10) one obtains

$$H(\kappa,t) = 1 + \sum_{n=0}^{\infty}\sum_{k=0}^{\infty} \frac{(n+k)!\,(\|\kappa\|^2\, Dt^{\alpha})^{n+1}(-c^2 D^{-1} t^{\beta})^{n+k+1}}{n!\,k!\,\Gamma[\beta(n+k+1)+\alpha(n+1)+1]},$$

and using $m = n + k$ as index of summation,

$$H(\kappa,t) = 1 - \|\kappa\|^2\, c^2 t^{\alpha+\beta} \sum_{m=0}^{\infty}\sum_{n=0}^{m} \binom{m}{n} \frac{(-c^2 D^{-1} t^{\beta})^m (\|\kappa\|^2\, Dt^{\alpha})^n}{\Gamma(\beta m + \alpha n + \alpha + \beta + 1)},$$

which completes the proof. □

The following result gives another representation of the Fourier transform via a contour integral.

Theorem 2. *The Fourier transform* (9) *of the initial-value problem* (3) *and* (8) *is given by the formula*

$$H(\kappa,t) = \frac{1}{2\pi \mathrm{i}} \int_{\mathrm{Ha}} e^{\xi} \xi^{\alpha-1} \frac{\xi^{\beta} + c^2 D^{-1} t^{\beta}}{\xi^{\alpha+\beta} + c^2 D^{-1} \xi^{\alpha} t^{\beta} + \|\kappa\|^2\, c^2 t^{\alpha+\beta}}\, d\xi, \tag{13}$$

where Ha *is the Hankel contour.*

Proof. It follows from the contour integral representation of the reciprocal gamma function

$$\frac{1}{\Gamma(z)} = \frac{1}{2\pi \mathrm{i}} \int_{\mathrm{Ha}} \mathrm{e}^{\xi} \xi^{-z}\, d\xi,$$

that

$$H(\kappa,t) = \left[1 - \frac{\|\kappa\|^2\, c^2 t^{\alpha+\beta}}{2\pi \mathrm{i}} \int_{\mathrm{Ha}} \mathrm{e}^{\xi} \xi^{-(\alpha+\beta+1)} \sum_{m=0}^{\infty}\sum_{n=0}^{m} \binom{m}{n} (-c^2 D^{-1} t^{\beta} \xi^{-\beta})^m (\|\kappa\|^2\, Dt^{\alpha} \xi^{-\alpha})^n\, d\xi\right].$$

As the internal sum can be simplified as

$$\sum_{n=0}^{m} \binom{m}{n} (\|\kappa\|^2\, Dt^{\alpha} \xi^{-\alpha})^n = (1 + \|\kappa\|^2\, Dt^{\alpha} \xi^{-\alpha})^m,$$

then

$$H(\kappa,t)=1-\frac{\|\kappa\|^2 c^2 t^{\alpha+\beta}}{2\pi \mathrm{i}}\int_{\mathrm{Ha}} \mathrm{e}^{\xi}\xi^{-(\alpha+\beta+1)}\sum_{m=0}^{\infty}[(-c^2D^{-1}t^{\beta}\xi^{-\beta})(1+\|\kappa\|^2 Dt^{\alpha}\xi^{-\alpha})]^m\,d\xi.$$

It is convenient now to change the integration variable from ξ to $\rho=\xi/t$ (for $t>0$), that is,

$$H(\kappa,t)=\left[1-\frac{\|\kappa\|^2 c^2}{2\pi \mathrm{i}}\int_{\mathrm{Ha}} \mathrm{e}^{\rho t}\rho^{-(\alpha+\beta+1)}\sum_{m=0}^{\infty}\left[-c^2D^{-1}\frac{(\rho^{\alpha}+\|\kappa\|^2 D)}{\rho^{\alpha+\beta}}\right]^m\,d\rho\right].$$

If the contour is taken in a such a way that

$$\left|c^2D^{-1}\frac{(\rho^{\alpha}+\|\kappa\|^2 D)}{\rho^{\alpha+\beta}}\right|<1,$$

then it follows that

$$H(\kappa,t)=1-\frac{\|\kappa\|^2 c^2}{2\pi \mathrm{i}}\int_{\mathrm{Ha}}\frac{\mathrm{e}^{\rho t}\rho^{-1}}{\rho^{\alpha+\beta}+c^2D^{-1}\rho^{\alpha}+\|\kappa\|^2 c^2}\,d\rho.$$

Let us return to the ξ variable of the integration, that is,

$$H(\kappa,t)=1-\frac{\|\kappa\|^2 c^2 t^{\alpha+\beta}}{2\pi \mathrm{i}}\int_{\mathrm{Ha}}\frac{\mathrm{e}^{\xi}\xi^{-1}}{\xi^{\alpha+\beta}+c^2D^{-1}\xi^{\alpha}t^{\beta}+\|\kappa\|^2 c^2 t^{\alpha+\beta}}\,d\xi.$$

By the contour representation of the gamma function

$$1=\frac{1}{\Gamma(1)}=\frac{1}{2\pi \mathrm{i}}\int_{\mathrm{Ha}}\mathrm{e}^{\xi}\xi^{-1}\,d\xi$$

and therefore

$$H(\kappa,t)=\frac{1}{2\pi \mathrm{i}}\int_{\mathrm{Ha}}\frac{\mathrm{e}^{\xi}}{\xi}\left[1-\frac{\|\kappa\|^2 c^2 t^{\alpha+\beta}}{\xi^{\alpha+\beta}+c^2D^{-1}\xi^{\alpha}t^{\beta}+\|\kappa\|^2 c^2 t^{\alpha+\beta}}\right]\,d\xi,$$

which gives the representation (13). □

Example 1. *Let us consider the particular case when $\alpha=\beta$. In this case the denominator in* (13) *can be written as*

$$\xi^{2\alpha}+c^2D^{-1}t^{\alpha}\xi^{\alpha}+\|\kappa\|^2 c^2 t^{2\alpha}=(\xi^{\alpha}+A_{+}t^{\alpha})(\xi^{\alpha}+A_{-}t^{\alpha}),$$

where

$$A_{\pm} = \frac{c^2}{2D}(1 \pm \Omega), \qquad \Omega = \sqrt{1 - \frac{4\left\|\kappa\right\|^2 D^2}{c^2}}.$$

We also have

$$\frac{\xi^{\alpha} + c^2 D^{-1} t^{\alpha}}{(\xi^{\alpha} + A_{+} t^{\alpha})(\xi^{\alpha} + A_{-} t^{\alpha})} = \left(\frac{1+\Omega}{2\Omega}\right) \frac{1}{\xi^{\alpha} + A_{-} t^{\alpha}} - \left(\frac{1-\Omega}{2\Omega}\right) \frac{1}{\xi^{\alpha} + A_{+} t^{\alpha}}.$$

In this case the solution (13) *reduces to*

$$H(\kappa, t) = \left[\left(\frac{1+\Omega}{2\Omega}\right) \frac{1}{2\pi \mathrm{i}} \int_{Ha} e^{\xi} \xi^{\alpha-1} \frac{1}{\xi^{\alpha} + A_{-} t^{\alpha}} \, d\xi - \left(\frac{1-\Omega}{2\Omega}\right) \frac{1}{2\pi \mathrm{i}} \int_{Ha} e^{\xi} \xi^{\alpha-1} \frac{1}{\xi^{\alpha} + A_{+} t^{\alpha}} \, d\xi \right].$$

The contour integral representation of the one-parameter Mittag-Leffler function defined as $\mathrm{E}_{\alpha}(z) = \mathrm{E}^{1}_{\alpha,1}(z)$ *is*

$$\mathrm{E}_{\alpha}(z) = \frac{1}{2\pi \mathrm{i}} \int_{Ha} \frac{e^{\xi} \xi^{\alpha-1}}{\xi^{\alpha} - z} \, d\xi.$$

Then $H(\kappa, t)$ *can be given by*

$$H(\kappa, t) = \left(\frac{1+\Omega}{2\Omega}\right) \mathrm{E}_{\alpha}(-A_{-} t^{\alpha}) - \left(\frac{1-\Omega}{2\Omega}\right) \mathrm{E}_{\alpha}(-A_{+} t^{\alpha}),$$

which is the solution obtained in [24].

Remark 1. *The inverse Fourier transform of* (13) *has an independent interest.*

The Fourier transform $H(\kappa, t)$ *is given by* (13) *with initial condition* (11). *To calculate the inverse Fourier transform* $Q(x, t)$ *one has to compute the integral*

$$Q(x,t) = \frac{1}{(2\pi)^3} \int_{\mathbb{R}^3} e^{-\mathrm{i}\langle \kappa, x \rangle} \frac{A}{B + \left\|\kappa\right\|^2} \, d\kappa = \frac{1}{2\pi^2 r} \int_0^{\infty} \frac{A\mu \sin(\mu r)}{B + \mu^2} \, d\mu,$$

where $r = \left\|x\right\|$ *and* $\mu = \left\|\kappa\right\|^2$. *Indeed*

$$q(x,t) = \frac{1}{2\pi \mathrm{i}} \int_{Ha} e^{\xi} \xi^{\alpha-1} \left(\xi^{\beta} + c^2 D^{-1} t^{\beta}\right) \mathcal{F}^{-1} \left[\frac{1}{\xi^{\alpha+\beta} + c^2 D^{-1} \xi^{\alpha} t^{\beta} + \left\|\kappa\right\|^2 c^2 t^{\alpha+\beta}} \right] d\xi$$

and

$$\mathcal{F}^{-1}\left[\frac{1}{\xi^{\alpha+\beta}+c^2D^{-1}\xi^{\alpha}t^{\beta}+\|\kappa\|^2c^2t^{\alpha+\beta}}\right]=\frac{1}{2\pi^2r}\int_0^{\infty}\frac{\mu\sin(\mu r)}{\xi^{\alpha+\beta}+c^2D^{-1}\xi^{\alpha}t^{\beta}+\mu^2c^2t^{\alpha+\beta}}\,dk$$
$$=\frac{1}{2\pi^2rc^2t^{\alpha+\beta}}\int_0^{\infty}\frac{\mu'\sin\mu'(r/ct^{(\alpha+\beta)/2})}{\xi^{\alpha+\beta}+c^2D^{-1}\xi^{\alpha}t^{\beta}+\mu'^2}\,d\mu'.$$

This integral can be evaluated using

$$\int_0^{\infty}\frac{\mu\sin(a\mu)}{b^2+\mu^2}\,dk=\frac{\pi}{2}\mathrm{e}^{-ab},$$

with $a>0$ *and* $\mathrm{Re}\,b>0$*, which gives*

$$Q(x,t)=\frac{1}{2\pi\mathrm{i}}\frac{1}{4\pi rc^2t^{\alpha+\beta}}\int_{Ha}e^{\xi}\xi^{\alpha-1}\left(\xi^{\beta}+c^2D^{-1}t^{\beta}\right)e^{-\frac{r\xi^{\alpha/2}}{ct^{(\alpha+\beta)/2}}\sqrt{\xi^{\beta}+cD^{-1}t^{\beta}}}\,d\xi.$$

The function $H(\kappa,t)=H(\|\kappa\|,t)$, $\kappa\in\mathbb{R}^3$, $t\geq 0$, given by (9) is radial. We will use the same notation for function $H(\mu,t),\mu=\|\kappa\|\geq 0$, $t\geq 0$.

Theorem 3. *Let us assume that for every* $t\geq 0$

$$\int_0^{\infty}\mu^2\left|H(\mu,t)\right|^2G(d\mu)<\infty, \tag{14}$$

where the finite measure G *is given by* (5)*.*

Then, the solution $q(x,t)=q(x,t,\omega)$, $x\in\mathbb{R}^3$, $\omega\in\Omega$, $t\geq 0$, *of initial-value problem* (3), (6) *can be written as the stochastic integral*

$$q(x,t)=\int_{\mathbb{R}^3}e^{\mathrm{i}\langle k,x\rangle}H(\kappa,t)Z(dk), \tag{15}$$

where $H(\kappa,t)$ *is given by* (9)*, and the random measure* $Z(\cdot)$ *is defined in* (6)*.*

The covariance function of the spatio-temporal random field (15) *is of the form*

$$\mathrm{Cov}(q(x,t),q(x',t))=\int_{\mathbb{R}^3}e^{\mathrm{i}\langle k,x-x'\rangle}H(\kappa,t)H(k,t')F(dk), \tag{16}$$

where the spectral measure F *is defined by* (6)*.*

Proof. If q is defined in (9), then by (15) it holds

$$\begin{aligned} q(x,t) &= \int_{\mathbb{R}^3} \eta(y)Q(x-y,t) = \int_{\mathbb{R}^3} \eta(x-z)Q(z,t)dz \\ &= \int_{\mathbb{R}^3} e^{\mathrm{i}\langle k,x\rangle}\left[\int_{\mathbb{R}^3} e^{\mathrm{i}(k,-z')}Q(z,t)dz\right]Z(dk) = \int_{\mathbb{R}^3} e^{\mathrm{i}\langle k,x\rangle}H(\kappa,t)Z(dk), \end{aligned}$$

where all stochastic integrals exist in $\mathscr{L}_2(\Omega)$ sense. □

3 Angular Time-Dependent Power Spectrum

Consider the unit radius sphere $\mathbf{S}^2 = \{x \in \mathbb{R}^3 : \|x\| = 1\}$ that is centred at the origin with the surface Lebesque measure $\sigma(dx) = \sigma(d\theta, d\varphi) = \sin\theta d\theta d\varphi$, $\theta \in [0,\pi]$, $\varphi \in [0, 2\pi]$.

A spatio-temporal spherical random field defined on a probability space $(\Omega, \mathcal{F}, \mathrm{P})$ is a random function $T(x,t) = T(x,t,\omega) = T(\theta,\varphi,t)$, $x \in \mathbf{S}^2$, $t \geq 0$.

We consider a real-valued spatio-temporal spherical random field T with zero mean and finite second-order moment which is continuous in the mean-square sense, see [29, p.9] for definitions and other details.

We assume that the random field T is second-order isotropic, that is $\mathrm{E}[T(x,t)T(y,t')] = \mathrm{E}[T(\mathbf{g}x,t)T(\mathbf{g}y,t)]$ for every $\mathbf{g} \in SO(3)$, where $SO(3)$ denotes the group of rotation in $\mathbb{R}^3$. This is equivalent to the condition that the covariance function $\mathrm{E}[T(\theta,\varphi,t)T(\theta',\varphi',t')]$ depends only on the angular distance $\gamma = \gamma_{PP'}$ between two points $P = (\theta,\varphi)$ and $P' = (\theta',\varphi')$ on $\mathbf{S}^2$ for every $t, t' \geq 0$.

Under these conditions, the random field T can be expanded in the mean-square sense as the Laplace series

$$T(\theta,\varphi,t) = \sum_{l=0}^{\infty}\sum_{m=-l}^{l} Y_{lm}(\theta,\varphi)g_{lm}(t),$$

where the functions $Y_{lm}(\theta, \varphi)$ represents the complex spherical harmonics and the coefficients $g_{lm}(t)$ are complex-valued stochastic processes defined by

$$g_{lm}(t) = \int_0^{\pi} \int_0^{2\pi} T(\theta, \varphi, t) \overline{Y_{lm}(\theta, \varphi)} \sin\theta d\theta d\varphi,$$

and

$$\mathrm{E} g_{lm}(t) \overline{g_{l'm'}(t')} = \delta_{ll'} \delta_{mm'} C_l(t, t'),\ -l \leq m \leq l,\ -l' \leq m' \leq l',\ l, l' = 0, 1, 2, \ldots.$$

The functional series $\{C_l(t, t'),\ l = 0, 1, 2, \ldots\}$ is called the angular time-dependent power spectrum of the isotropic random field $T(\theta, \varphi, t)$ on $\mathbf{S}^2$. For every $t, t' \geq 0$ it satisfies the condition

$$\sum_{l=0}^{\infty} (2l+1) C_l(t, t') < \infty.$$

Then, a covariance function between two locations with the angular distance γ at times t and t' is equal

$$R(\cos\gamma, t, t') = \mathrm{E}[T(\theta, \varphi, t) T(\theta', \varphi', t')] = \frac{1}{4\pi} \sum_{l=0}^{\infty} (2l+1) C_l(t, t') P_l(\cos\gamma),$$

where

$$P_l(x) = \frac{1}{2^l \cdot l!} \frac{d^l}{dx^l} (x^2 - 1)^2$$

is the l-th Legendre polynomial.

The random field $q(x, t)$, $x \in \mathbb{R}^3$, $t \geq 0$, given by (15) is homogeneous and isotropic in x. Hence, using the addition theorem for Bessel functions, its covariance function (16) can be

written in the form

$$\begin{aligned}\mathrm{Cov}(q(x,t),q(x',t')) &= \int_0^\infty \frac{\sin(\mu\,\|x-x'\|)}{\mu\,\|x-x'\|}H(\mu,t)H(\mu,t')G(d\mu)\\ &= 2\pi^2\sum_{l=0}^{\infty}\sum_{m=-l}^{l} Y_{lm}(\theta,\varphi)\overline{Y_{lm}(\theta',\varphi')}\\ &\times \int_0^\infty \frac{J_{l+1/2}(\mu r)}{(\mu r)^{1/2}}\cdot\frac{J_{l+1/2}(\mu r')}{(\mu r')^{1/2}}H(\mu,t)H(\mu,t')G(d\mu),\end{aligned}$$

where (r,θ,φ) and (r',θ',φ') are spherical coordinates of $x\in\mathbb{R}^3$ and $y\in\mathbb{R}^3$ respectively.

Using the Karhunen theorem [23, p.10] one obtains the following spectral representation of homogeneous and isotropic random field in $\mathbb{R}^3$:

$$q(x,t)=q(r,\theta,\varphi,t)=\pi\sqrt{2}\sum_{l=0}^{\infty}\sum_{m=-l}^{l}Y_{lm}(\theta,\varphi)\int_0^\infty\frac{J_{l+1/2}(\mu r)}{(\mu r)^{1/2}}H(\mu,t)Z_{lm}(d\mu), \tag{17}$$

where the random measures $Z_{lm}(\cdot)$ are defined in (7).

The restriction of the homogeneous and isotropic random field (17) to the sphere $\mathbf{S}^2$ is an isotropic spherical random field $T_H(x,t)$, $x\in\mathbf{S}^2$, $t\geq 0$, which will be called a spherical fractional hyperbolic diffusion random field (SFHDRF).

In this case

$$\mathrm{Cov}(T_H(x,t),T_H(x',t'))=R(\cos\gamma,t,t')=\int_0^\infty\frac{\sin(2\mu\sin\left(\frac{\gamma}{2}\right))}{2\sin\left(\frac{\gamma}{2}\right)}H(\mu,t)H(\mu,t')G(d\mu), \tag{18}$$

where the Euclidean distance $\|x-x'\|$ (also called the chordal distance between two points $x,x'\in\mathbf{S}^2\subset\mathbb{R}^3$) can be expressed in terms of the great circle (also known as geodesic or spherical) distance as follows: $\|x-x'\|=2\sin(\gamma/2)$, $\gamma=\gamma(x,x')=\arccos(\langle x,x'\rangle)$.

By addition theorem for spherical Bessel functions, the isotropic random field $T_H(x,t)$, $x\in\mathbf{S}^2$, $t>0$, has the following spectral representation:

$$T_H(x,t)=\sum_{l=0}^{\infty}\sum_{m=-l}^{l}Y_{lm}(\theta,\varphi)a_{lm}^H(t), \tag{19}$$

with the stochastic processes

$$a_{lm}^H(t) = \pi\sqrt{2}\int_0^\infty \frac{J_{l+1/2}(\mu r)}{(\mu r)^{1/2}} H(\mu,t) Z_{lm}(d\mu),\ t \geq 0. \tag{20}$$

Thus, the angular spectrum of the SFHDRF in (19) is of the form

$$C_l(t,t') = \mathrm{E} a_{lm}^H(t)\overline{a_{lm}^H(t')} = 2\pi^2 \int_0^\infty \frac{J_{l+1/2}^2(\mu)}{\mu} H(\mu,t)H(\mu,t')G(d\mu),\ l = 0,1,2,\ldots, \tag{21}$$

where

$$\begin{aligned} H(\mu,t) &= 1 + \sum_{n=0}^{\infty} \left(-\mu^2 c^2 t^{\alpha+\beta}\right)^{n+1} \mathrm{E}_{\beta,(\alpha+\beta)(n+1)-1}^{n+1}\left(-\frac{c^2}{D}t^\beta\right) \\ &= 1 - \mu^2 c^2 t^{\alpha+\beta} \sum_{m=0}^{\infty}\sum_{n=0}^{\infty} \binom{m}{n} \frac{\left(-\frac{c^2}{D}t^\beta\right)^m (\mu^2 D t^\alpha)^n}{\Gamma(\beta m + \alpha n + \alpha + \beta + 1)}. \end{aligned} \tag{22}$$

We can summarise the above results as the following theorem, which is the main result of the paper.

Theorem 4. *Under the condition* (14) *the SFHDRF in* (19) *is an isotropic random field on* $\mathbf{S}^2$ *with the angular power spectrum given by formulae* (21) *and* (22).

Example 2. *Consider the Matérn class of covariance functions for the initial condition* (5) *which has the following form:*

$$\mathrm{E}\eta(x)\eta(x') = \sigma^2 \frac{2^{1-\nu}}{\Gamma(\nu)} \left(a\left\|x - x'\right\|\right)^\nu K_\nu(a\left\|x-x'\right\|),\ x, x' \in \mathbb{R}^3,$$

where $\sigma^2 > 0$, $a > 0$, *and* K_ν *is the modified Bessel function of the second kind of order* $\nu > 0$. *This class found numerous applications in statistics and machine learning, see, for example,* [26], [34], *and references therein.*

Then, the spectral measure G *in* (5) *has the isotropic spectral density* $g(\mu)$ *defined by* $G'(\mu) = 4\pi\mu^2 g(\mu)$, *which is equal*

$$g(\mu) = \frac{\sigma^2 \Gamma(\nu + \frac{3}{2}) a^{2\nu}}{\pi^{3/2}\Gamma(\nu)} \frac{1}{(a^2+\mu^2)^{\nu+\frac{3}{2}}},\ \mu \geq 0.$$

Here, the parameter ν controls the degree of differentiability of random field $\eta(x), x \in \mathbb{R}^3$, which represent the initial condition (5)*, σ is field's variance and the parameter a is the scale parameter.*

Thus, condition (14) *is equivalent to*

$$\int_0^\infty \frac{\mu^2}{(a^2+\mu^2)^{\nu+\frac{3}{2}}} \left|H(\mu,t)\right|^2 d\mu < \infty,$$

for every $t \geq 0$. It is satisfied for $\alpha = \beta \in (0,1]$, see [24] *for details, and for general $1 < \alpha + \beta \leq 2$ for $\nu > 0$.*

Let us consider the partial case of the initial-value problem (3), (4)*, when $\alpha = \beta \in (0,1]$. Then, see Remark* 1,

$$H(\mu,t) = \left(\frac{1+\Omega}{2\Omega}\right) \mathrm{E}_\alpha(-A_- t^\alpha) + \left(\frac{1-\Omega}{2\Omega}\right) \mathrm{E}_\alpha(-A_+ t^\alpha) =$$

$$= \frac{1}{2}(\mathrm{E}_\alpha(-A_- t^\alpha) + \mathrm{E}_\alpha(-A_+ t^\alpha)) + \frac{1}{2\Omega}(\mathrm{E}_\alpha(-A_- t^\alpha) - \mathrm{E}_\alpha(-A_+ t^\alpha)),$$

where

$$A_\pm = A_\pm(\mu) = \frac{c^2}{2D}(1 \pm \Omega),$$

$$\Omega = \Omega(\mu) = \sqrt{1 - \frac{4\mu^2 D^2}{c^2}} = \sqrt{1 - \frac{4\mu^2 D^2}{c^2}}\, \mathbf{1}_{\mu \leq c/2D} + \mathrm{i}\sqrt{\frac{4\mu^2 D^2}{c^2} - 1}\, \mathbf{1}_{\mu > c/2D},$$

and $\mathbf{1}_{\{\}}$ denotes the indicator function.

This case was considered in [24]*. The case $\alpha = 1$, $\alpha + \beta = 2$ is also known, see* [4], [21], [22]*, since $\mathrm{E}_1(z) = e^z$, and then*

$$\mathrm{E}_1(A_\pm) = \exp\left\{-\frac{c^2 t}{2D}(1 \pm \Omega)\right\},$$

which gives

$$H(\mu,t) = \exp\left\{-\frac{c^2t}{2D}\right\}\left\{\left[\cosh\left(ct\sqrt{\frac{c^2}{4D^2}-\mu^2}\right)+\frac{c}{2D\sqrt{\frac{c^2}{4D^2}-\mu^2}}\sinh\left(ct\sqrt{\frac{c^2}{4D^2}-\mu^2}\right)\right]\mathbf{1}_{\mu\le c/2D}\right.$$
$$\left. + \left[\cos\left(ct\sqrt{\mu^2-\frac{c^2}{4D^2}}\right)+\frac{c}{2D\sqrt{\mu^2-\frac{c^2}{4D^2}}}\sin\left(ct\sqrt{\mu^2-\frac{c^2}{4D^2}}\right)\right]\mathbf{1}_{\mu>c/2D}\right\},$$

and the angular spectrum

$$C_l(t,t') = 2\pi^2\left[\int_0^{\frac{c}{2D}}\frac{J^2_{l+1/2}(\mu)}{\mu}\bar{H}_1(\mu,t)\tilde{H}_1(\mu,t')G(d\mu)+\int_{\frac{c}{2D}}^{\infty}\frac{J^2_{l+1/2}(\mu)}{\mu}\bar{H}_2(\mu,t)\tilde{H}_2(\mu,t')G(d\mu)\right],$$

where

$$\bar{H}_1(\mu,t) = \exp\left\{-\frac{c^2t}{2D}\right\}\left[\cosh\left(ct\sqrt{\frac{c^2}{4D^2}-\mu^2}\right)+\frac{c}{2D\sqrt{\frac{c^2}{4D^2}-\mu^2}}\sinh\left(ct\sqrt{\frac{c^2}{4D^2}-\mu^2}\right)\right]\mathbf{1}_{\mu\le c/2D},$$
$$\bar{H}_2(\mu,t) = \exp\left\{-\frac{c^2t}{2D}\right\}\left[\cos\left(ct\sqrt{\mu^2-\frac{c^2}{4D^2}}\right)+\frac{c}{2D\sqrt{\mu^2-\frac{c^2}{4D^2}}}\sin\left(ct\sqrt{\mu^2-\frac{c^2}{4D^2}}\right)\right]\mathbf{1}_{\mu>c/2D}.$$

4 Numerical studies

This section numerically investigates the solution $T_H(x,t)$ and its spectral and covariance properties with respect to parameters α and β. Two examples similar to those presented in [4] (where the case of $\alpha=\beta=1$ was considered) are used to study the impact of α and β.

We use the approach developed in [4], see the justifications and detailed discussions there. However, the numerical analysis in this paper requires more sophisticated approximation methods compared to [4]. Namely, a much more general case of two fractional derivatives of the orders α and β is considered. Thus, in this general case, the function $H(\mu,t)$ is not given via elementary functions and for computations one has to use a truncated version of

the series (22). Figure 1 uses the truncated double series with 80 m and n terms to illustrate the dependence of $H(\mu, t)$ on its parameters. The first subplot in Figure 1 shows $H(1, 0.1)$ for $\alpha, \beta \in [0.5, 1]$. The second subplot illustrates changes of $H(\mu, t)$ with respect to its arguments $\mu \in [1, 20]$ and $t \in [0, 1]$ for the fixed values of parameters $\alpha = 0.8$ and $\beta = 1$. In the bottom row $H(1, t)$ is shown as a functions of t and α or β for fixed $\beta = 1$ and $\alpha = 0.5$ respectively. The plots illustrate that, as a general trend, the functions $H(\mu, t)$ exhibit a decreasing behaviour as their parameters α and β decrease. Furthermore, there is a decline of $H(\mu, t)$ with increasing values of time t. Increasing the value of μ introduces a decaying oscillatory behaviour.

Note that, similar to [4], there are no explicit elementary functional relations between $C_l(t, t')$, $R(\cos\gamma, t, t')$ and $C_l(0, 0)$, $R(\cos\gamma, 0, 0)$ respectively. To compute spectral and covariance functions of $T_H(x, t)$ at time $t > 0$ one has to approximate the integral representations (18), (20) and (21) that use the spectral measure $G(\cdot)$ and stochastic measures $Z_{lm}(\cdot)$ of the initial random condition field $\eta(x)$.

In the following examples we illustrate the obtained results by using simulated data with the covariance function and oscillating angular spectrum that are similar to those observed for the CMB data, see plots and discussions in [4]. In the examples we assume that the measure $G(\cdot)$ is discrete with a finite support set. Absolutely continuous spectral measures can be approximated by selecting a sufficiently a large dense support set.

Let us denote by $\{\mu_i,\ i = 1, \ldots, I\}$ the support of $G(\cdot)$ and its values by

$$\sigma_i^2 = G(\mu_i) = \mathbf{E}\ Z_{lm}^2(\mu_i),\ i = 1, \ldots, I,$$

where $Z_{lm}(\cdot)$ are real-valued random variables. Under the assumptions that the random field

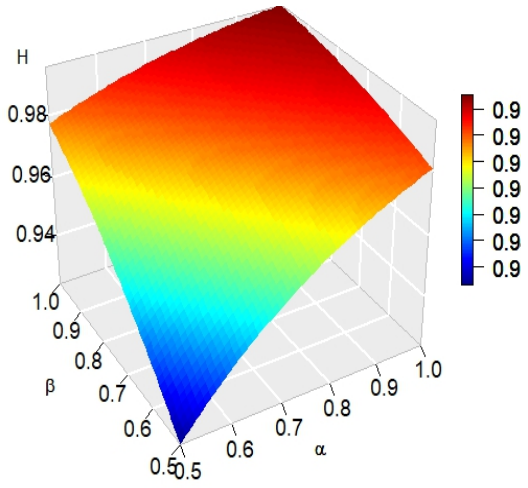

(a) $H(1, 0.1)$ as a function of α and β

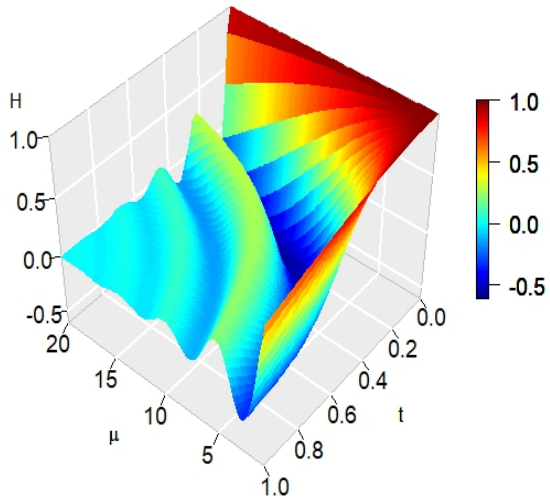

(b) $H(\mu, t)$ for fixed $\alpha = 0.8$ and $\beta = 1$

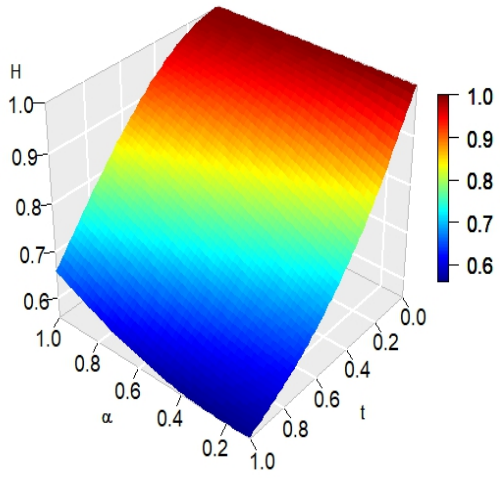

(c) $H(1, t)$ as a function of t and α when $\beta = 1$

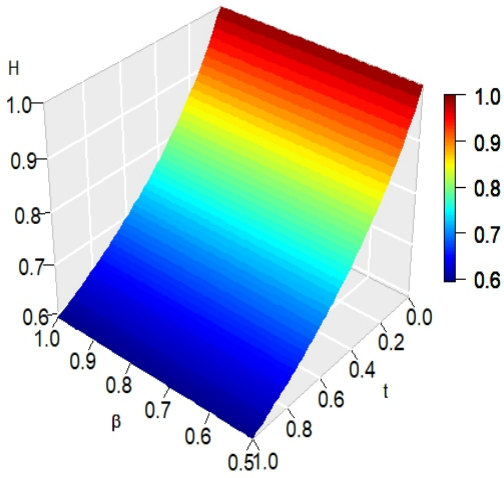

(d) $H(1, t)$ as a function of t and β when $\alpha = 0.5$

Figure 1: Dependence of $H(\mu, t)$ on its parameters and arguments

$\eta(x)$ is centered Gaussian, the random variables $Z_{lm}(\mu_i) \sim N(0, \sigma_i^2)$ and independent for different l, m and i.

Then, formulae (18), (20) and (21) take the following discrete forms

$$R(\cos\gamma,t,t')=\sum_{i=1}^{I}\frac{\sin(2\mu_i\sin(\frac{\gamma}{2}))}{2\mu_i\sin(\frac{\gamma}{2})}\tilde{H}(\mu_i,t)\tilde{H}(\mu_i,t')\sigma_i^2, \tag{23}$$

$$a_{lm}(t)=\pi\sqrt{2}\sum_{i=1}^{I}\frac{J_{l+\frac{1}{2}}(\mu_i)}{\sqrt{\mu_i}}\tilde{H}(\mu_i,t)Z_{lm}(\mu_i),$$

$$C_l(t,t')=2\pi^2\sum_{i=1}^{I}\frac{J^2_{l+\frac{1}{2}}(\mu_i)}{\mu_i}\tilde{H}(\mu_i,t)\tilde{H}(\mu_i,t')\sigma_i^2. \tag{24}$$

Example 3. *This example illustrates changes over time of the covariance function* $R(\cos\gamma,t,t)$ *and the power spectrum* $C_l(t,t)$. *The parameters* $c=1$ *and* $D=1$ *in equation* (3) *were selected. To produce plots and computations we used the corresponding discrete equations* (23) *and* (24) *with the spectrum support* $\mu_i=1+4(i-1)$ *and values* $\sigma_i=100/i$, $i\in\{1,2,\ldots,10\}$, *i.e.* $I=10$. *To compute approximate values of the functions* $H(\mu,t)$ *we used truncated double series in* (22) *with 80 terms for both* n *and* m. *The empirical studies show that increasing the number of terms does not change the plots.*

For the cases of $\alpha=\beta=1$ *and* $\alpha=0.8$, $\beta=1$, *Figure* 2 *show the covariance* $R(\cos\gamma,t,t)$ *at the time lags* $t=0,\ t=0.1$ *and* $t=0.5$ *as functions of the angular distance* γ. *As expected, the first subplot in Figure* 2 *coincides with the particular case considered in Example* 2 *and the corresponding plot in* [4, Figure 2a]. *The covariance plots in Figure* 2 *and results for the same* $t=0.1$ *but different values* α *and* β *in Figure* 3 *suggest that the variance of the field and dependencies at short angular distances decrease with decreasing values of* α *and* β. *At large angular distances dependencies are smaller and therefore their decrease has a smaller magnitude.*

To understand effects of the orders of fractional derivatives and the angular distance on the covariance function, we provide 3D-plots in Figure 4. *They show the covariance as functions*

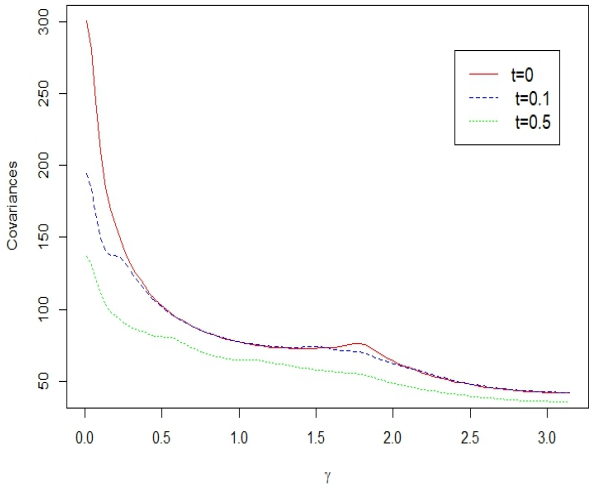

(a) The case of $\alpha = \beta = 1$

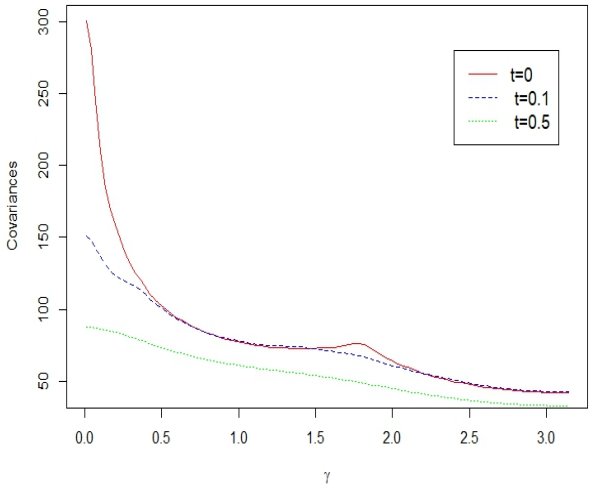

(b) The case of $\alpha = 0.8$ and $\beta = 1$

Figure 2: $R(\cos\gamma, t, t)$ at the time lags $t = 0,\ 0.1$, and 0.5 for $c = D = 1$

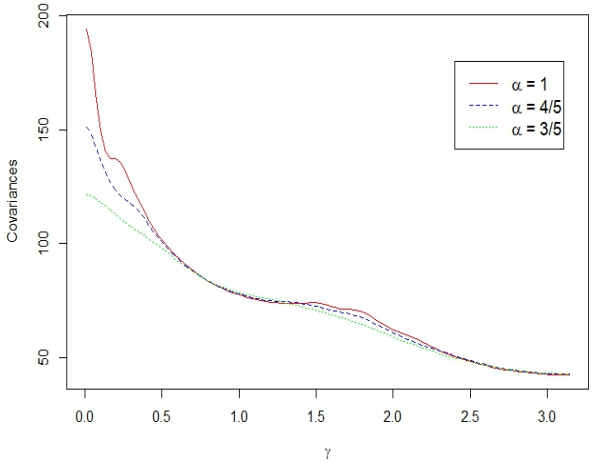

(a) The case of $\beta = 1$

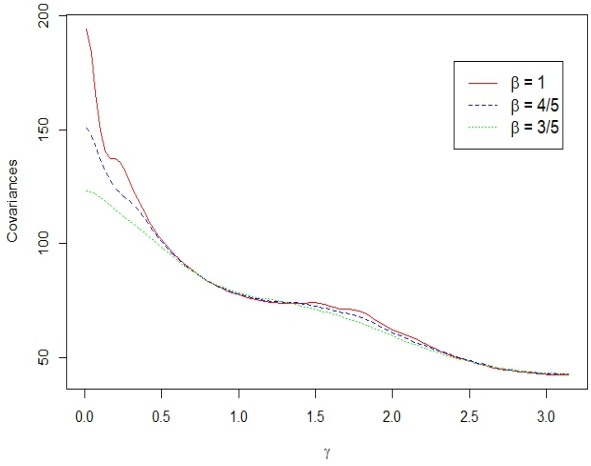

(b) The case of $\alpha = 1$

Figure 3: $R(\cos\gamma, t, t)$ at the time lag $t = 0.1$ for $c = D = 1$

of the angular distances γ *and the parameters* α *and* β*. The fixed numeric values* $\beta = 1$ *and* $\alpha = 0.8$ *of another fractional order were used for each of the subplots respectively. The values* $c = D = 1$ *and* $t = 0.1$ *were selected. The plots in Figure* 4 *were normalized by the*

maximum value of $R(\cos\gamma, 0.1, 0.1)$. *The plots suggest that the covariance decays when the angular distance increases and the fractional orders decrease. Moreover, it decreases faster with respect to decreasing* α *than* β.

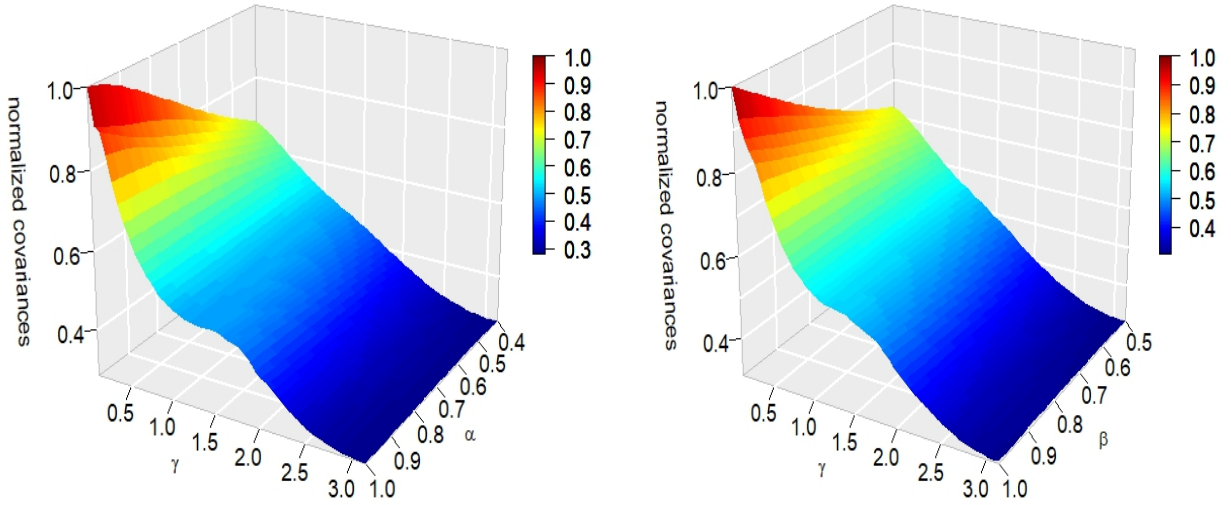

(a) $R(\cos\gamma, 0.1, 0.1)$ as a function of γ and α for $\beta = 1$ (b) $R(\cos\gamma, 0.1, 0.1)$ as a function of γ and β for $\alpha = 0.8$

Figure 4: $R(\cos\gamma, t, t)$ at the time lag $t = 0.1$ for $c = D = 1$

Figure 5 *displays the power spectrum* $C_l(t, t)$ *as a function of time* t *and the fractional orders* α *and* β. *To produce this figure we used the time interval* $t \in [0, 0.5]$ *and two sets of indices* $l = 2, 5, 10, 20$ *and* $l = 3, 6, 11, 21$. *Two combinations of orders of fractional derivatives,* $\alpha = 0.8,\ \beta = 1$ *and* $\alpha = 1,\ \beta = 0.8$, *were used. The plots demonstrate that the power spectrum magnitudes decay very quickly regardless of the values of* α *and* β *when* l *increases.*

Example 4. *In this numeric example we consider SFHDRF for the parameters* $c = 1$ *and* $D = 2$. *The initial condition random field* $\eta(\mathbf{x})$ *with low and high frequency components is studied. Namely, the support of its discrete spectrum belongs to the intervals* $[0, 20]$ *and* $[80, 90]$. *To simulate realisations of random fields at the same small scale as real CMB values*

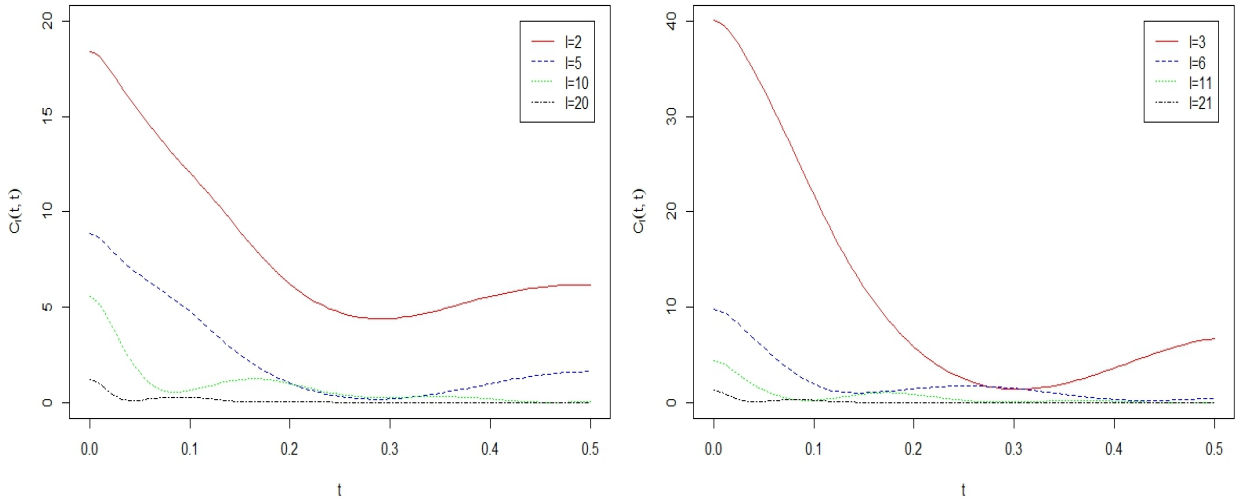

(a) $C_l(t,t)$ as a function of t for $\alpha = 0.8$ and $\beta = 1$ (b) $C_l(t,t)$ as a function of t for $\alpha = 1$ and $\beta = 0.8$

Figure 5: $C_l(t,t)$ on the interval $[0, 0.5]$ for $c = D = 1$

we use the values $\sigma_i^2 = 0.00003$ *and* 0.0001 *for low and high frequency components respectively.*

We use the CMB tools and colour palettes from the R package rcosmo [18] *and the Python package healpy for fast computations of Healpix images from the corresponding Laplace series. As approximations of spherical fields we use Laplace series with the first* 100 *coefficients* C_l *obtained by applying* (24) *to the above discrete spectrum. The plots in Figure* 6 *show the angular power spectrum coefficients* $C_l(t,t)$ *at the specific time instances* $t = 0, 0.05$ *and* 0.1 *for different values of alpha and beta. The magnitude of these coefficients exhibits a decreasing trend as time* t *progresses and as the values of* α *and* β *decrease.*

The first map in Figure 7 *shows the initial condition random field i.e.* $T_H(x, 0)$ *computed for* $t = 0$*. Then, maps are presented for* $t = 0.05$ *and various combinations of parameters* α *and* β*. The obtained plots suggest that with increasing* t *the field is getting smother, which is expected from general physical and cosmological arguments. Also, it is evident from the maps*

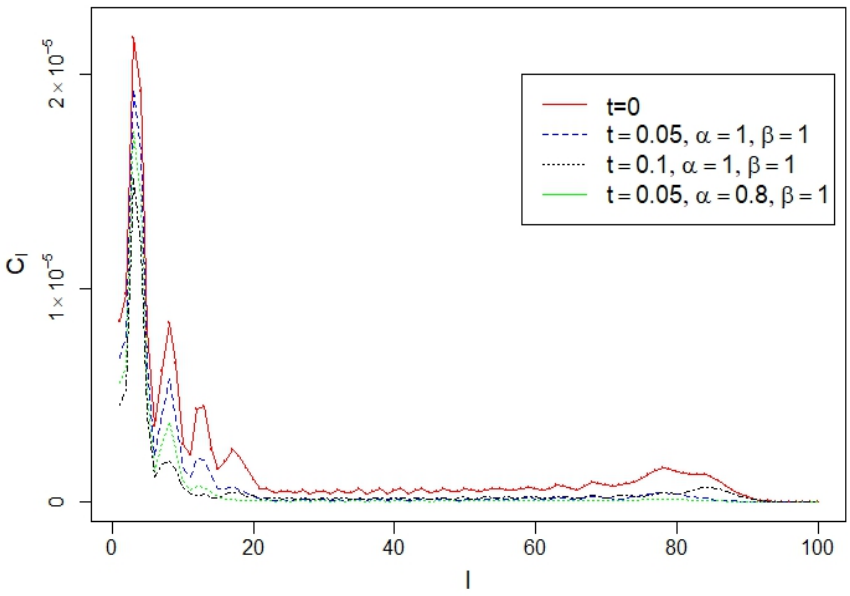

Figure 6: $C_l(t,t)$ for $c = D = 1$

that smaller values of the orders of fractional derivatives make temporal fields smoother.

References

[1] Adam, R., et al.: Planck 2015 results. I. (2016) Overview of products and scientific results. Astron. Astrophys. **594**, A16.

[2] Bouchaud, J.-P., and Georges, A. (1990) Anomalous diffusion in disordered media: Statistical mechanisms, models and physical applications. Phys. Rep. **195**, 127-293.

[3] Broadbrige, P., Kolesnik, A., Leonenko, N., and Olenko, A. (2019) Random spherical hyperbolic diffusion, Journal of Statistical Physics, **177** (5), 889-916.

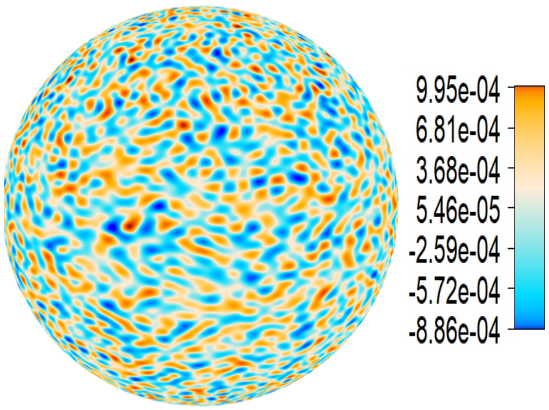

(a) The case of $t = 0$, $\alpha = 1$ and $\beta = 1$

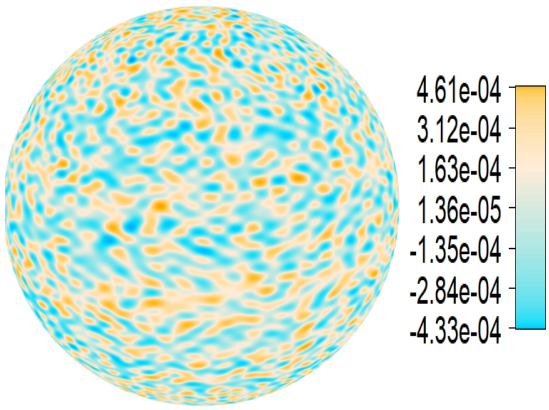

(c) The case of $t = 0.05$, $\alpha = 1$ and $\beta = 1$

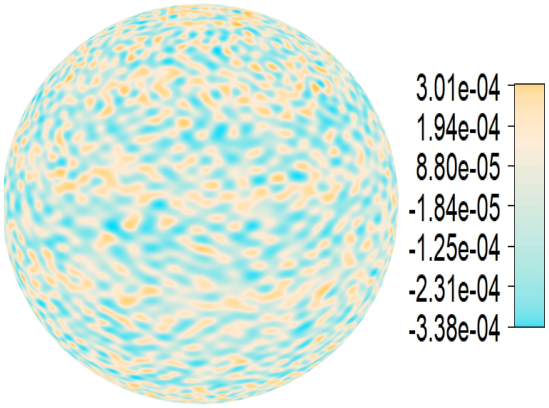

(e) The case of $t = 0.05$, $\alpha = 0.8$ and $\beta = 1$

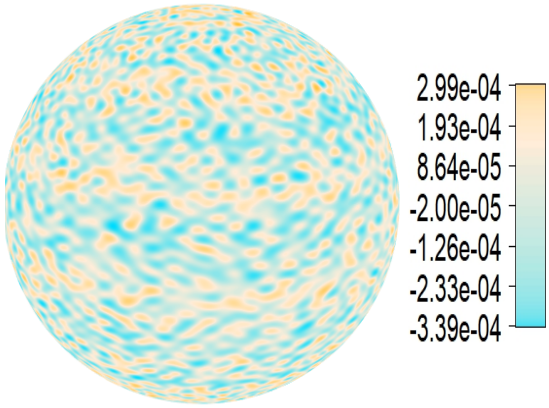

(g) The case of $t = 0.05$, $\alpha = 1$ and $\beta = 0.8$

Figure 7: SFHDRF $T_H(x, t)$ for $c = 1$ and $D = 2$.

[4] Broadbrige, P., Kolesnik, A., Leonenko, N., and Olenko, A. (2020) Spherically restricted random hyperbolic diffusion, Entropy, **22** (2) Paper N 217, 31pp.

[5] Broadbrige, P., Nanayakkara, R., and Olenko, A. (2022). On multifractionality of spherical random fields with cosmological applications, The ANZIAM Journal, **64** (2), 90-118.

[6] Cabella, P., and Marinucci, D. (2009) Statistical challenges in the analysis of cosmic microwave background radiation. Ann. Appl. Stat. **3**, 61-95.

[7] Cattaneo, C.R. (1958) Sur une forme de l'équation de la chaleur éliminant le paradoxe d'une propagation instantanée. Comptes Rendus **247**, 431-433.

[8] Christakos, G. (1992) Random Field Models in Earth Sciences. Academic Press, Inc., San Diego.

[9] Christakos, G. (2017) Spatiotemporal Random Fields: Theory and Applications. Elsevier, Amsterdam.

[10] Compte, A., and Metzler, R. (1997) The generalized Cattaneo equation for the description of anomalous transport processes. J. Phys. A: Math. Gen. **30**, 7277-7289.

[11] Del-Castillo-Negrete, D. (2008) Fractional diffusion models of anomalous transport, in Anomalous Transport: Foundations and Applications, Klages, R., Radons, G., Sokolov, I. M. (eds.), Wiley-VCH Verlag GmbH, Weinheim.

[12] Dodelson, S. (2003) Modern Cosmology. Academic Press, New York.

[13] D'Ovidio, M., Leonenko, N., and Orsingher, E. (2016) Fractional spherical random fields. Statist. Probab. Lett., **116**, 146–156.

[14] D'Ovidio, M., Orsingher, E., and Toaldo, B., (2014) Time-changed processes governed by space-time fractional telegraph equations, Stoch. Anal. Appl., **32**, 1009-1045.

[15] Figueiredo, C.R., Capelas de Oliveira, E., and Vaz, J. Jr. (2012) On the generalized Mittag-Leffler function and its application in a fractional telegraph equation. Math. Phys. Anal. Geom. **15** (1), 1-16.

[16] Fisher, N.I., Lewis, T., and Embleton, B.J.J. (1993) Statiscal Analysis of Spherical Data. Cambridge University Press, Cambridge.

[17] Fryer, D., Li, M., and Olenko, A. (2020) rcosmo: R Package for Analysis of Spherical, HEALPix and Cosmological Data. The R Journal. **12** (1), 206-225.

[18] Fryer, D.; Olenko, A.; Li, M.; and Wang, Yu. rcosmo: Cosmic Microwave Background Data Analysis. R package version 1.1.3. `https://CRAN.R-project.org/package=rcosmo`, **2021**.

[19] Gorenflo, R., Kilbas, A.A., Mainardi, F. and Rogosin, S.V., (2014) Mittag-Leffler Functions, Related Topics and Applications, Springer, Heidelberg.

[20] Ivanov, A.V. and Leonenko, N.N, (1989) Statistical Analysis of Random Fields, Kluwer Academic Publisher, Dordrecht.

[21] Kolesnik, A.D., (2021) Markov Random Flights, CRC Press, Boca Raton.

[22] Kolesnik, A.D. and Ratanov, N., (2022) Telegraph Process and Option Pricing, Springer, Berlin.

[23] Leonenko, N.N., (1999) Limit Theorems for Random Fields with Singular Spectrum. Kluwer Academic Pablisher, Dordrecht.

[24] Leonenko, N.N. and Vaz, J., (2020) Spectral analysis of factional hyperbolic diffusion equations with random data, Journal of Statistical Physics, **179**, 155-175.

[25] Leonenko, N., Nanayakkara, R. and Olenko, A. (2021) Analysis of spherical monofractal and multifractal random fields, Stochastic Environmental Research and Risk Assessment, **35**, 681–701.

[26] Leonenko, N.N., Malyarenko, A. and Olenko, A., (2022) On spectral theory of random fields in the ball, Theory Probab. and Math. Statist, **107**, 61-76.

[27] Mainardi, F. (2010) Fractional Calculus and Waves in Linear Viscoelasticity. Imperial College Press, London.

[28] Malyarenko, A., and Ostoja-Starzewski, M. (2019) Tensor-valued Random Fields for Continuum Physics. Cambridge University Press, Cambridge.

[29] Marinucci, D. and Peccati, G., (2011) Random Fields on the Sphere: Representation, Limit Theorems and Cosmological Applications, Cambridge University Press, Cambridge.

[30] Meerschaert, M. M., and Sikorskii, A. (2019) Stochastic Models for Fractional Calculus. Walter de Gruyter & Co., Berlin.

[31] Oh, H.-S., and Li, T.-H. (2004) Estimation of global temperature fields from scattered observations by a spherical-wavelet-based spatially adaptive method. J. R. Statist. Soc. B, **66**, 221-238.

[32] Orsingher, E. and Beghin, L., (2004), Time-fractional telegraph equations and telegraph processes with brownian time, Probab. Theory Relat. Fields, **128** (1), 141-160.

[33] Podlubny, I., (1999) Fractional Differential Equations, Academic Precc, New York.

[34] Porcu, E., Bevilacqua, M., Schaback, R., and Oates, C.J. (2023) The Matérn model: A journey through statistics, numerical analysis and machine learning, arXiv: 2303.02759.

[35] Povstenko, Y. and Ostoja-Starzewski, M. (2022) Fractional telegraph equation under moving time-harmonic impact, International Journal of Heat and Mass Transfer, **182,** 121958.

[36] Saxena, R.K., Garra, R. and Orsingher, E., (2015) Analytical solution of space-time fractional telegraph-type equations involving Hilfer and Hadamar derivatives, Integral Transform and Special Functions, **27** (1), 30-42.

[37] Weinberg, S. (2008) Cosmology. Oxford University Press, Oxford.